DALTON
FULL PAPER

Characterisation of defective silicalites †

Silvia Bordiga,[a] Irene Roggero,[a] Piero Ugliengo,[a] Adriano Zecchina,*[a] Vera Bolis,[b] Gilberto Artioli,[c] Roberto Buzzoni,[d] Gianluigi Marra,[d] Franco Rivetti,[d] Guido Spanò[d] and Carlo Lamberti[e]

[a] *Dipartimento di Chimica IFM Università di Torino, via P. Giuria 7, I-10125 Torino, Italy. E-mail: zecchina@ch.unito.it*
[b] *Dipartimento di Scienze Chimiche, Alimentari, Farmaceutiche e Farmacologiche Università del Piemonte Orientale "Amedeo Avogadro", Viale Ferrucci 33, 28100 Novara, Italy*
[c] *Dipartimento di Scienze della Terra, Università di Milano, via Botticelli 23, I-20133 Milano, Italy*
[d] *EniChem S.p.A. Centro Ricerche Novara, Istituto G. Donegani, via G. Fauser 4, I-28100, Novara, Italy*
[e] *Dipartimento di Chimica IFM Università di Torino, via P. Giuria 7, I-10125 Torino, Italy and Unità INFM di Torino Università, Italy*

Received 12th June 2000, Accepted 19th July 2000
First published as an Advance Article on the web 10th October 2000

The structure and the adsorptive properties of internal defects in two chemically very pure silicalite samples, characterised by a high and low concentration of defects (internal SiOH nests generated by Si vacancies), are investigated by means of several physical methods (neutron diffraction, IR spectroscopy of adsorbed NH_3, microcalorimetry of NH_3 adsorption and quantum chemical computation). The role of cooperative effects in hydrogen bonded chains and rings of silanols covering the internal defective nanocavities in influencing the absorptive properties of the material is elucidated. This study provides an explanation of the less hydrophobic character of defective silicalite relative to perfect silicalite and sheds light on the reason why defective silicalite acts as an efficient and selective catalyst for the gas phase Beckman rearrangement reaction where cyclohexanone oxime is converted into caprolactam.

Introduction

Silicalite, discovered by the group of Flanigen,[1] is a purely siliceous microporous material, representing the Si/Al $\longrightarrow \infty$ limit of the ZSM-5 zeolite.[2] It belongs to the large and growing family of MFI type structures. Silicalites obtained following the original patent [1a] exhibit a consistent concentration of Na and Al impurities which act as mineralising agents and the resulting crystals have a large monoclinic structure (2000–3500 nm). Its surface being almost completely internal and formed almost entirely by Si–O–Si bonds, perfect silicalite is inert and hydrophobic.

In EniChem laboratories silicalite samples with consistent different peculiarities [3] have been obtained, following the same synthesis procedure adopted for TS-1.[4] From a chemical point of view, all the silicalite samples prepared in this way exhibit a very high purity level, the amount of Na and Al impurities being as low as a few ppm. The absence of these mineralising agents results, upon calcination, in extremely small orthorhombic crystals (220–260 nm, see ref. 3(*a*)). Moreover, the silicalite samples contain a high amount of internal defects due to silicon vacancies. It is a matter of fact that a measurable increase in the pore volume over that of perfect silicalite has been observed for silicalites prepared following the EniChem method.[3a] Defective silicalites show a high density of internal OH groups, located in internal cavities. These data, taken together, have been interpreted as indirect proof of the presence of clustered vacancies, generating rather large internal hydroxylated nanocavities, also called hydroxyl nests. In fact, the substitution of an isolated Si atom by four OH groups does not increase the channel volume and the removal of several adjacent T sites is required to explain the volumetric results.

The synthesis method outlined above, allows us to obtain a family of silicalite samples characterised by defect concentrations (and hence of hydroxyl nests) varying over a wide range. In this contribution we shall focus our attention on two samples (denoted Sil–A and Sil–B) which can be considered as representative of two limiting situations, *i.e.* those characterised by a high defect concentration (Sil–A) and those characterised by a low defect concentration (Sil–B).

Coming to the properties of defective silicalites, we draw attention to the fact that, because of the presence of these hydroxylated nanocavities, this porous material is less hydrophobic than a perfect silicalite and shows interesting catalytic properties in reactions where a very mild acidity is needed. It is a matter of fact that defective silicalite is found to act as an efficient and selective catalyst for the Beckman rearrangement reaction performed in the gas phase,[5] where cyclohexanone oxime is converted into caprolactam.

Finally, it is worth underlining that defective silicalite is not only interesting because of its mild acidic properties, but also because the internal hydroxylated nanocavities can be used to graft heteroatoms and because the internal silanols, covering the nanocavity walls, give (upon outgassing at $T > 700$ K) strained and reactive Si–O–Si bridges.[7]

In order to identify in greater detail the location and properties of silanols in the internal nests of these pure silicalites, we have performed a combined structural, spectroscopic, calorimetric and theoretical investigation on two representative samples (Sil–A and Sil–B) characterised by high and low defect concentrations respectively. The results obtained on these samples are compared with those obtained on non-microporous amorphous silica samples containing high and low densities of surface SiOH groups.

Results and discussion

Neutron diffraction study

The first studies on defective silicalites were carried out by our

† Based on the presentation given at Dalton Discussion No. 3, 9–11th September 2000, University of Bologna, Italy.

Electronic supplementary information (ESI) available: colour version of Fig. 1. See http://www.rsc.org/suppdata/dt/b0/b004794p/

DOI: 10.1039/b004794p

group in 1992.[3] From what was learnt in that work, it emerged that, in order to better understand the properties of defective silicalites and in order to construct reasonable models for the theoretical computations, it was imperative to know whether or not the Si vacancies occur randomly among the 12 independent T sites of the MFI framework.

To answer this question we have recently performed a neutron powder diffraction study[6] on a Sil-A sample at the HRPD instrument of the ISIS pulsed neutron source. The measured data have been analysed using three different refinement strategies finalised to determine if some T sites show an occupancy significantly lower than unity. It has been found that the refinement of the T site occupancy factors consistently converged to similar results, independently of the assumed strategy. In particular, the occupancy factors of sites Si(6), Si(7), Si(10), and Si(11) systematically converged to values in the range 0.69–0.78, with mean values around 0.75(5). The site occupancy factors of all other tetrahedral sites were refined to values in the range 0.88–1.13, that is to say full occupancy within 3 esd.[6] Such values were consistently obtained independent of the assumed atomic displacement parameters (freely refinable or fixed), of the starting parameter set, and of the refinement strategy. On this basis, it has been concluded that the refined low occupancy factors of the Si(6), Si(7), Si(10), and Si(11) tetrahedral sites are considered as possible evidence of long range ordering of Si vacancies.[6]

The fact that three out of the four observed defective T sites are adjacent to each other (Si(7)–O(35)–Si(7), Si(7)–O(34)–O(11), Si(10)–O(22)–Si(11), Si(10)–O(38)–Si(10)) implies that, in principle, vacancy clusters consisting of up to 6 Si defects are possible (*i.e.* Si(7)–Si(7)–Si(11)–Si(10)–Si(10)–Si(11) loop). This is in agreement with the model of hydroxyl nests in silicalite put forward on the basis of spectroscopic and volumetric evidence. In fact, it can explain: (i) the increased adsorption properties of defective silicalites, not accounted for by isolated T vacancies;[3a] (ii) the presence of a broad band in the O–H stretching region due to SiOH groups interacting *via* hydrogen bonds (see refs. 3 and *vide infra*) and (iii) the appearance, in samples dehydrated at 773 K or higher, of bands in the skeleton stretching mode region around 900 cm^{-1} associated with strained Si–O–Si bridges formed by water elimination by vicinal silanols (see refs. 7 and *vide infra*). As a matter of fact, the elimination of some OH groups from selected defective T sites makes such strained Si–O–Si bridges possible.

This neutron diffraction study gave us, for the first time, direct structural evidence that internal OH groups in the Sil-A sample are clustered, forming rather large cavities inside the MFI channels. A pictorial representation of a possible hydroxyl nest distribution is reported in Fig. 1, where six adjacent Si(7)–Si(7)–Si(11)–Si(10)–Si(10)–Si(11) sites have been omitted. This particular cluster generates an hydroxyl nest containing twelve OH groups.

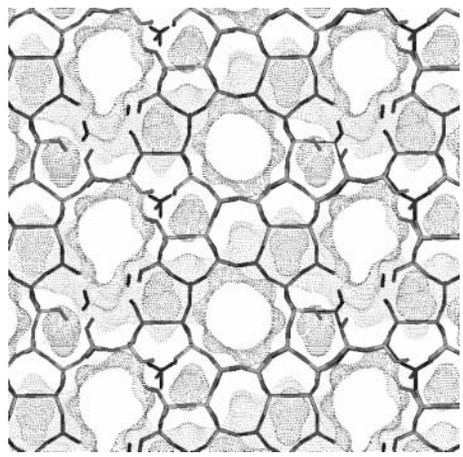

Fig. 1 Model of a possible hydroxyl nest inside a defective silicalite as inferred from the neutron diffraction data of ref. 6, where six adjacent T7, T10 and T11 sites have been omitted. This nest is composed of 12 SiOH groups.

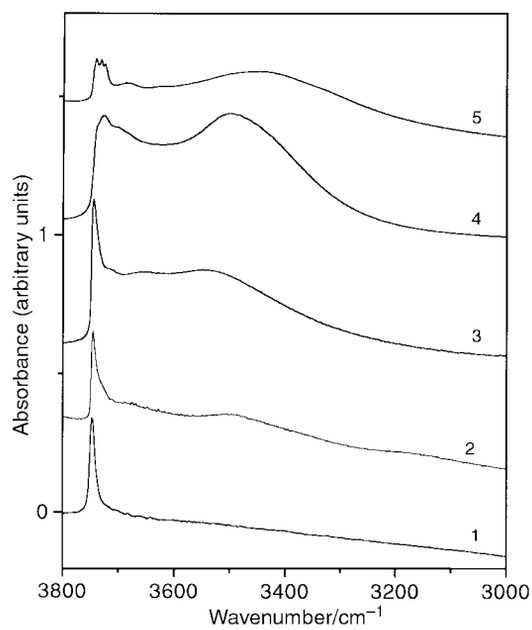

Fig. 2 IR spectra, collected at rt, from bottom to top of: a silica sample degassed at 973 K (curve 1); a Sil-B sample degassed at 973 K (curve 2); a silica sample degassed at 273 K (curve 3); a Sil-A sample degassed at 673 K (curve 4); and a Sil-B sample degassed at 673 K (curve 5).

IR Spectroscopy of isolated and H-bonded silanols

From the extremely abundant literature on the subject (see *e.g.* refs. 3, 7–10 and references therein), it is well known that the IR spectroscopy of silanols is characterised by absorptions in the 3750–3000 cm^{-1} range. In particular, free species are associated with narrow ν(OH) bands in the 3750–3700 cm^{-1} range while, hydroxyls mutually interacting *via* medium-strength hydrogen bonds, are associated with broad bands at lower frequency. These features can be observed either in amorphous (such as SiO_2 silica gel) and in crystalline materials (such as quartz and zeolites). The abundance of one species with respect to the others is related to the sample nature, with the synthesis and post-synthesis treatments and with the thermal activation conditions.

In Fig. 2 the infrared spectra in the 3800–3000 cm^{-1} range of a non-porous high surface area silica sample (Aerosil) and of two silicalites (Sil-A and Sil-B) are compared as a function of the activation temperature. Curve 1 corresponds to a silica sample degassed at 973 K: in this IR spectrum we observe a single sharp and nearly symmetric peak at 3747 cm^{-1} readily assigned to the ν(OH) of isolated silanols located on external surfaces (Scheme 1).

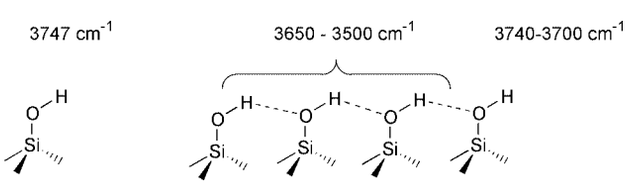

Scheme 1

Curve 2 reports the IR spectrum of Sil-B degassed at the same temperature. In this case: we note a more complex spectrum because the main peak, centered at 3745 cm^{-1}, shows a clear shoulder at lower frequency at about 3720 cm^{-1}. This component has been associated with isolated silanols located at

internal positions. The IR spectrum obtained on a silica sample degassed at room temperature, (a treatment allowing the complete removal of physisorbed water) is reported as curve 3. We observe the presence of a very complex spectrum characterised by many components in the 3750–3500 cm^{-1} range. In particular the sharp band, centered at 3745 cm^{-1}, is associated with isolated species while the three components at 3711, 3655 and 3540 cm^{-1} are associated with silanol groups in terminal positions (3711 cm^{-1}) or involved in H-bonded chains of increasing length (3655 and 3540 cm^{-1}: see Scheme 1). We tentatively assign the band at 3655 cm^{-1} to dimers and the band at 3540 cm^{-1} to trimers and oligomers of higher nuclearity. Curve 4 has been obtained on a Sil-A sample degassed at 673 K. The obtained spectrum is definitively more intense and more complex then that of silica, showing strong and composite absorptions in a very large spectroscopic range: 3750–3300 cm^{-1}. In particular the maximum at 3747 cm^{-1} (characteristic of isolated silanol on external surfaces) does not appear as a distinct component, because it is overshadowed by a very complex absorption covering the 3750–3700 cm^{-1} interval. The components forming the envelope (3710–3680 cm^{-1}) are assigned to nearly free hydroxyl groups (either isolated or in terminal positions) located in internal sites. On this basis the strong band centered at ≈3500 cm^{-1} and the shoulder at about 3450 cm^{-1} can be associated with a high concentration of H-bonded silanols in internal defects probably forming linear and ring chains. The high intensity of this absorption, in Sil-A, can be rationalized by the presence of a high concentration of internal hydroxylated cavities in the zeolite framework (nests). This IR evidence is in full agreement with the picture emerging from the neutron diffraction data (*vide supra*). Finally curve 5 reports the spectrum obtained for Sil-B activated at 673 K. By comparing the intensities of curves 5 and 4 we observe that the concentration of SiOH groups in the Sil-B sample is much lower. From the shape of the spectra, we observe essentially the same kind of silanol bands in both samples, however the components are better separated in curve 5, indicating that the defects present in Sil-B exhibit a higher structural definition and a higher order with respect to those present in Sil-A. In particular, the better defined spectrum shows distinct components in the free (nearly free) silanols spectral range (characteristic triplets of well resolved maxima at 3742, 3732 and 3725 cm^{-1}) while as far as the H-bonded spectral region is concerned a clear component is observed at 3680 cm^{-1} and a strong and complex band is now centred at 3420 cm^{-1}. The complex nature of this band is evidenced by lowering the temperature: in fact the broad shoulder observed at 3680 cm^{-1} at room temperature shows, after cooling, a composite structure (peaks at 3641 and 3667 cm^{-1}), while the intense absorption centred at 3420 cm^{-1} (at rt) separates into three well defined components at about 3500, 3400 and 3300 cm^{-1}.[7]

IR spectroscopy of dehydrated samples interacting with NH_3

The adsorption at rt of increasing doses of NH_3 on silica and Sil-B, both activated at 973 K, are compared in Fig. 3. The results obtained in both experiments are, in general terms, very similar and for this reason will be described together. Two spectroscopic "anomalies" observed for Sil-B will then be discussed.

Upon NH_3 adsorption the band associated with the isolated or nearly isolated silanols is progressively consumed due to the formation of hydrogen bonded species following Scheme 2.

These new species are characterised by a low OH stretching mode frequency absorbing over a large range: with a maximum around 3100 ($\Delta\nu$(OH) = −650 cm^{-1}), and 2900 cm^{-1} ($\Delta\nu$(OH) = −850 cm^{-1}) for silica and Sil-B respectively: characteristic of strong H-bond formation. On Sil-B the maximum at lower $\bar{\nu}$ (2900 *vs.* 3100 cm^{-1}) is definitively more pronounced than on silica: this suggests that hydrogen bonds formed inside the internal nanovoids of defective silicalite are stronger, and

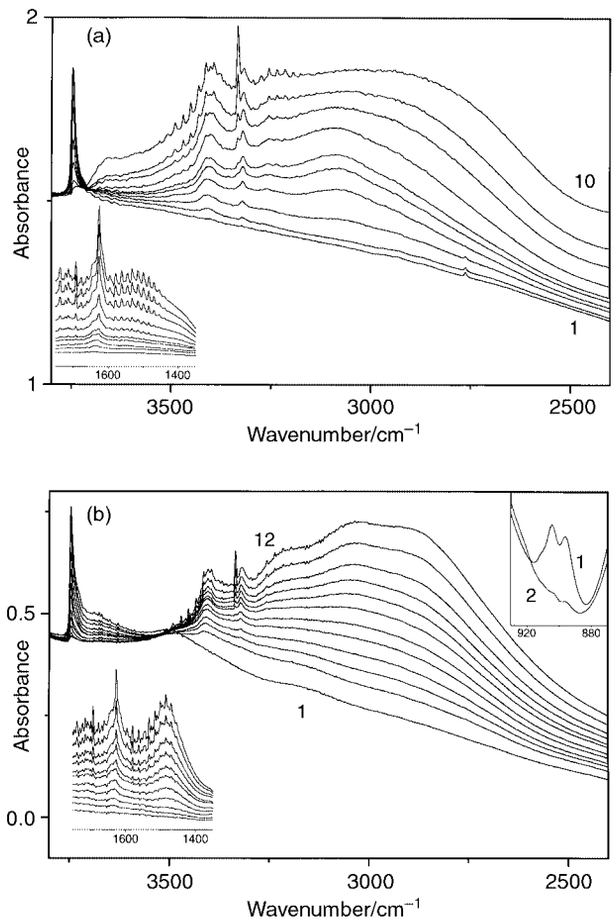

Fig. 3 IR spectra in the ν(OH) and ν(NH) stretching region, collected at rt, of increasing doses of ammonia dosed on silica and on Sil-B (both samples degassed at 973 K) parts (a) and (b) respectively. The insets in the left bottom corner of both parts report the spectra in the δ(OH) and δ(NH) bending regions. The inset in the top right corner of part (b) reports the effect of the first NH_3 dosage on the skeleton Si–O–Si bands in the 910–880 cm^{-1} range. First spectrum in vacuum, remaining spectra in the range 0.5–70 Torr.

better defined, than those occurring on the surface of amorphous silica. Upon increasing the NH_3 equilibrium pressure (P_{NH_3}), the rather sharp N–H stretching bands of adsorbed ammonia molecules are clearly observed at 3405 and 3320 cm^{-1}, ν_{asym}(NH) and ν_{sym}(NH) respectively. The interaction with the surface causes, for both bands, a bathochromic shift of 9 and 15 cm^{-1} with respect to the unperturbed molecule. The intrinsic weakness of the NH···H hydrogen bond among ammonia molecules explains why the ν_{sym}(NH) of NH_3 molecules in the condensed state is so close to that observed in the gas phase (3335 cm^{-1}). A further P_{NH_3} increase causes the appearance of a sharp band at 3334 cm^{-1}, very close to the ν_{sym}(NH) of NH_3 in the gas phase. The same behaviour is observed in the δ(N–H) bending region, reported in the insets (left bottom corner in Fig. 3): δ(NH) = 1635 cm^{-1} at low P_{NH_3}, with evolution of a sharp component at δ(NH) = 1628 cm^{-1}, the same frequency as in the gas phase, for the highest coverages. As in this pressure range, the hydroxyl groups have been completely consumed, the NH_3 adsorption is of the multilayer type.

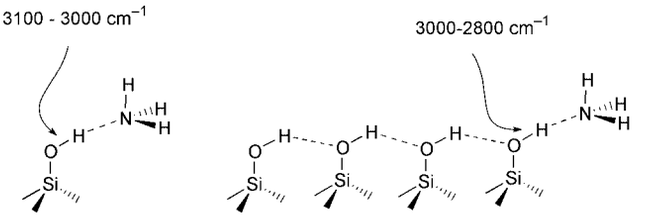

Scheme 2

The fact that the last adsorbed ammonia molecules are not directly interacting with silanols is witnessed by the fact that the last spectra undergoes a consistent modification in the 3300–2500 cm^{-1} range even if silanols have already been nearly completely consumed. This means that the formation of ad-layers of liquid-like NH_3 physisorbed on the previously described species is accompanied by perturbation of the ν(OH) mode of the $SiOH \cdots NH_3$ adducts of the first monolayer. As a consequence, when comparison will be made between experimental and computed $\Delta\bar{\nu}$(OH) values, the experimental data should refer to the low coverage spectra, where the formation of a liquid-like phase is not yet present.

We now come to discuss the two spectral features characteristic of the Sil-B sample only. The first dose of ammonia is already able to completely remove the bands in the 910–880 cm^{-1} range (inset in the right top corner of Fig. 3b). As these bands have been assigned to strained Si–O–Si bridges, abundantly formed upon silanol condensation at 973 K, this result indicates that the strained Si–O–Si bridges have been opened by NH_3 following the pathway depicted in Scheme 3.

Scheme 3

Looking again in the δ(NH) stretching region, we observe (inset in the left bottom corner of Fig. 3b) that a strong and rather broad band, centred at 1480 cm^{-1}, develops on Sil-B upon increasing P_{NH_3}. This spectroscopic feature is rather surprising, since it appears in the stretching region where the δ(NH) of NH_4^+ is expected.[11] A complex band is always found in this region upon dosing NH_3 onto protonic zeolites due to the protonation reaction. However, if the proton transfer to ammonia is an expected phenomenon on H-zeolites, the rather low Brønsted acidity of silanols in silicalite seems insufficient to justify such a conclusion in our case. It is worth noting that, at the highest P_{NH_3} values, a less intense (and much broader) band also develops on silica at about 1520 cm^{-1} (inset in the left bottom corner of Fig. 3a). For the time being, we shall not try a complete assignment of this band, because further experiments with ND_3 are needed to clarify the attribution.

Fig. 4 reports the same experiment performed on silica degassed at RT, and on Sil-A activated at 673 K. The comparison of the spectra of the two samples, treated at different temperatures, is suggested by the fact that, after these treatments, both samples show a high concentration of hydrogen bonded silanols forming long interacting chains (either linear or ring type). Interaction with ammonia results in a complete removal of the isolated silanol band and in a substantial reduction of the bands of the H-bonded OH groups with the parallel growth of a broad band in the 3400–2600 cm^{-1} range. The spectra reported in Fig. 4 are rather complex, since several parallel or mutually interconnected phenomena are simultaneously occurring. In particular the formation of $SiOH \cdots NH_3$ adducts involves: (i) isolated silanols; (ii) terminal silanols at the end of H-bonded linear silanol chains of different length; (iii) silanols of the same chains located in internal positions; (iv) H-bonded silanols of ring chains (likely to be particularly abundant on Sil-A). Finally, at the highest P_{NH_3} values, where most silanols are already engaged, a further evolution of the spectra (due to perturbation of the ν(OH) mode of the $SiOH \cdots NH_3$ adducts upon formation of ad-layers of liquid-like ammonia) is observed, as was the case for the spectra reported in Fig. 3.

The formation of $SiOH \cdots NH_3$ adducts on isolated silanols is responsible for the formation of a band similar to that observed on samples activated at higher temperatures (*i.e.* around 3100 cm^{-1}, *vide supra* Fig. 3). The interaction with terminal silanols is expected to be associated with a greater perturbation of the ν(OH) band, due to the cooperative effect

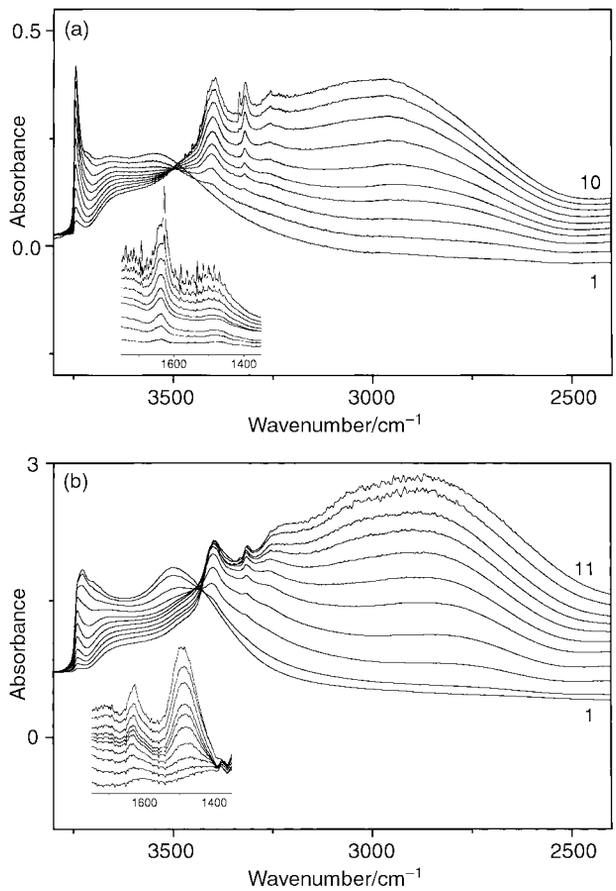

Fig. 4 IR spectra in the ν(OH) and ν(NH) stretching region, collected at rt, of increasing doses of ammonia dosed on silica (activated at rt) and on Sil-A (degassed at 673 K) parts (a) and (b) respectively. The insets in the left bottom corner of both parts report the spectra in the δ(OH) and δ(NH) bending regions. First spectrum in vacuum, remaining spectra in the range 0.5–70 Torr.

of the chain. We ascribe the maximum at about 2900 cm^{-1} ($\Delta\nu$(OH) = −850 cm^{-1}), observed in Fig. 4a for silica, to the ν(OH) of $SiOH \cdots NH_3$ adducts formed on terminal silanols involved in H-bonded chains longer than three units (*vide infra* for the computational part). The same phenomenon results, in the Sil-A sample, in an even more shifted band: ν(OH) ≈ 2800 cm^{-1} ($\Delta\nu$(OH) ≈ −950 cm^{-1}). The main structural differences between these two highly hydroxylated samples is due to the presence, in Sil-A nests, of closed chains of interacting silanols forming a loop, as suggested by the neutron data. We ascribe this higher shift to the direct insertion of ammonia in H-bonded silanol rings. This hypothesis will be confirmed by the computational study (*vide infra*).

By increasing P_{NH_3}, the absorption of ammonia on SiOH groups located inside chains (and/or polyaddition of ammonia in rings) is occurring. This is associated with the chain (ring) break and in the subsequent smaller red shifts of all involved OH groups due to the reduction of the cooperative effects in chains of smaller length (or rings). As a consequence, the high coverage spectra become similar to those observed on the samples activated at higher temperature and containing prevalently isolated silanols (see Fig. 3).

Coming to the ν(NH) bands, we observe that ammonia adsorbed on silanol chains has the same ν_{asym}(NH) and ν_{sym}(NH) frequencies as observed on samples with a low OH density (see Fig. 3). This indicates that the ν(NH) modes are not very much influenced by hydrogen bonding involving the N atom.

As far as the δ(NH) region is concerned (see inset of Fig. 4a,b), we observe, on both samples, the already discussed band at 1638 cm^{-1} ascribed to the bending modes of NH_3 adsorbed on silanols (broad at low P_{NH_3}). At higher P_{NH_3} a sharper band

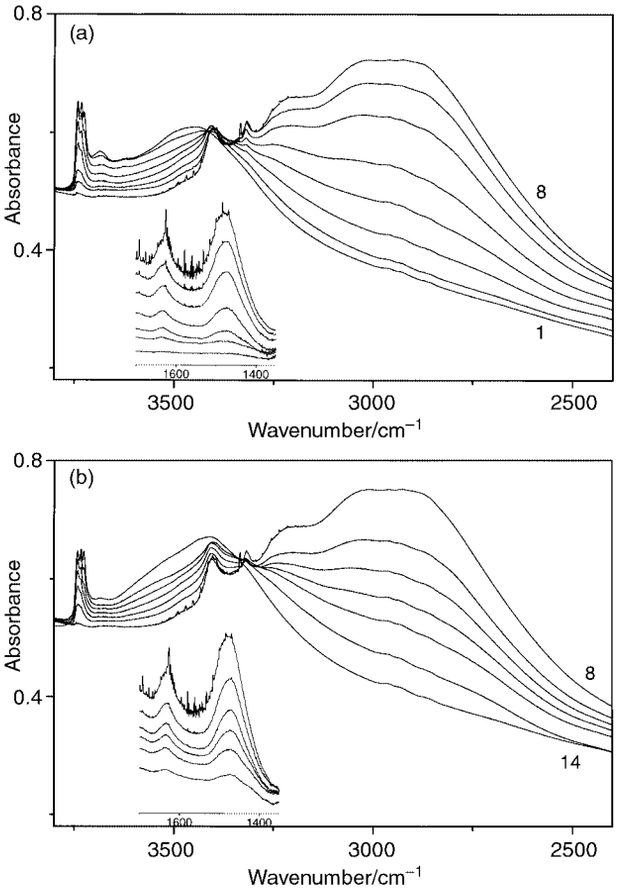

Fig. 5 IR spectra in the ν(OH) and ν(NH) stretching region, collected at rt, of ammonia on Sil-B (activated at 673 K): parts (a) and (b) report spectra obtained upon increasing and decreasing P_{NH_3} respectively. The insets in the left bottom corner of both parts report the spectra in the δ(OH) and δ(NH) bending regions. First spectrum in vacuum, spectra 2–8 in the range 0.5–70 Torr, spectra 8–14 in the range 70–0 Torr.

at 1628 cm^{-1} appears, which is due to NH_3 in secondary layers or in the gas phase. The unassigned band at lower frequency is clearly present in both highly hydroxylated samples, at 1484 cm^{-1} on Sil-A (more intense) and at 1490 cm^{-1} on silica.

The same experiment performed on the Sil-B sample activated at 673 K is reported in Fig. 5a, while Fig. 5b shows the spectra obtained in the subsequent degassing experiment. In the previous cases, the results of the degassing experiment at rt were not reported since they indicated a complete reversibility of ammonia binding. The main spectroscopic features resulting from this experiment are similar to those obtained and already described for Sil-A (Fig. 4b) since in this case we also observe, upon NH_3 contact, the progressive erosion of silanol bands and the parallel formation of a very broad absorption extending in the 3400–2600 cm^{-1} range. The only substantial difference with Sil-A lies in the nearly total disappearance of the bands of interacting H-bonded silanols in chains and/or rings. This indicates that, although the SiOH concentration in Sil-B is much lower than in Sil-A, all groups can directly be engaged by ammonia. Although the exact location of the maximum of the band formed upon interaction with ammonia is not straightforward (because of the broad character of the absorption), it seems that silanols of Sil-B are even more perturbed than silanols of Sil-A: we tentatively locate the maximum at ν(OH) ≈ 2750 cm^{-1} ($\Delta\nu$(OH) ≈ −1000 cm^{-1}). As already mentioned in the discussion of Fig. 2, the Sil-B sample activated at 673 K shows a remarkably resolved triplet of bands in the region of free (or nearly free) silanols (maxima at 3742, 3732 and 3725 cm^{-1}) and a broad shoulder at 3680 cm^{-1} in the region of weakly bonded silanols. Among them, the first to be engaged by NH_3 are those absorbing at 3725 cm^{-1} and at 3680 cm^{-1}. This erosion

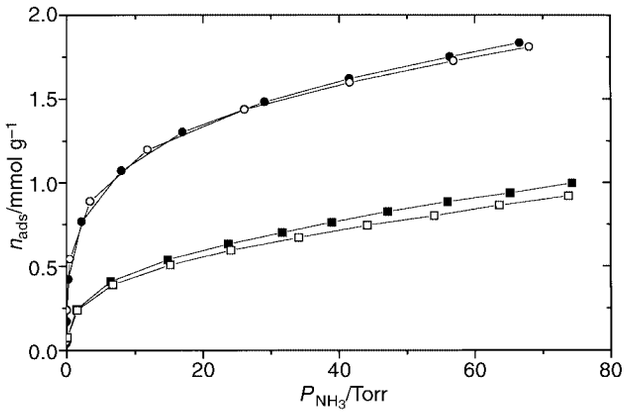

Fig. 6 Volumetric isotherms of NH_3 adsorbed at 303 K on Sil-A (circles) and on Sil-B (squares) silicalite. Solid symbols refer to the first, open symbols to the second run of adsorption.

is accompanied by the formation of the broad band with a maximum centred at 3450 cm^{-1}. Only afterwards the decrease of the 3732 and 3742 cm^{-1} bands is observed in succession.

The spectra in the ν(NH) (ν_{asym}(NH) at 3415 cm^{-1} and ν_{sym}(NH) at 3320 cm^{-1}) and δ(NH) (the low-wavenumber component is now observed at 1475 cm^{-1}) regions are similar to those observed on the sample degassed at higher temperature (Fig. 3b) and on Sil-A (Fig. 4b) and will not be commented upon further.

Upon reducing progressively the P_{NH_3}, the spectra reported in Fig. 5b were obtained. The first effect is the nearly total restoration of the components at 3742 and 3732 cm^{-1}. Further pressure decreases yield the partial restoration of the band at 3725 cm^{-1} and of the broad envelope centred at 3450 cm^{-1}. In no cases did we observe a significant restoration of the component at 3680 cm^{-1} (weakly bonded silanols). This indicates that NH_3 adsorption on Sil-B is not completely reversible at rt. The partial irreversibility of the process is also confirmed by the results obtained in the δ(NH) bending region (inset of Fig. 5b), where there is clear evidence that bands of NH_3 adsorbed are still present also after prolonged pumping at rt. This picture will be fully validated by the microcalorimetry study.

Microcalorimetry of NH_3 adsorption (first and second isotherms)

In Fig. 6 the volumetric isotherms (first and second runs) of the adsorption of NH_3 on the two silicalite specimens activated at 673 K are reported.

It is clearly evident that the amounts of NH_3 adsorbed per unit mass of the sample are much higher in the case of the highly defective Sil-A sample than in the case of Sil-B. By comparing the first and second run curves, it appears that the interaction NH_3/silicalite is almost completely reversible in the whole range of pressure examined (0–70 Torr), but for a little amount of ammonia that remains irreversibly held at the surface even after a prolonged degassing at rt. Indeed, the irreversible component is less than 2% of the total adsorption in the case of Sil-A and around 10% in the case of Sil-B. These data mean that the adsorption of NH_3 does not modify the surface site structure in the case of the Sil-A sample (2% is within the uncertainty of the experimental data), and only to a small extent in the case of the Sil-B. This fact agrees with the IR evidence, reported in Fig. 5, showing that the initial IR spectrum is not fully restored upon outgassing at rt. The nature of the sites irreversibly binding ammonia can be tentatively ascribed to highly energetic hydrogen bonds. Indeed the IR spectra have indicated, for the two silicalites, a higher $\Delta\nu$(OH) with respect to silica.

As mentioned before, the adsorption capacity is significantly higher in the case of the Sil-A sample, in agreement with the spectroscopic evidence in the OH stretching region (see Fig. 4b

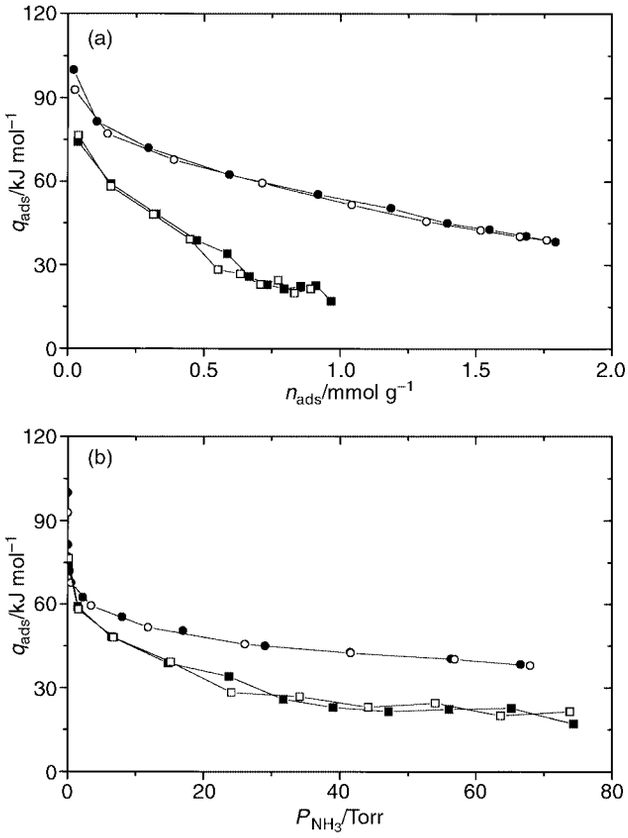

Fig. 7 Differential heat of adsorption (303 K) as a function of the amounts of NH_3 adsorbed (a) and as a function of the NH_3 equilibrium pressure (b), on Sil-A (circles) and Sil-B (squares). Solid symbols refer to the first, open symbols to the second run of adsorption.

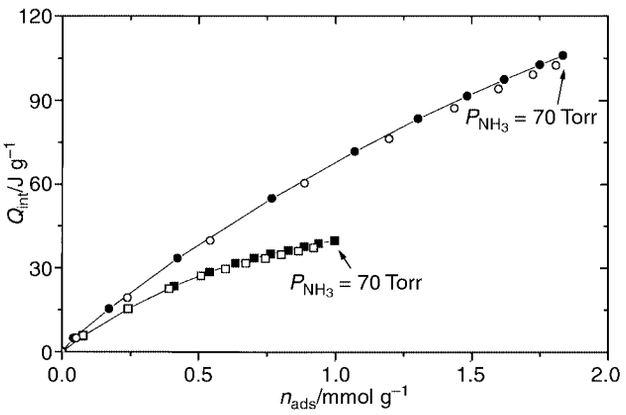

Fig. 8 Integral heat of adsorption (303 K) as a function of amounts of NH_3 adsorbed, on Sil-A (circles) and Sil-B (squares) silicalite. Solid symbols refer to the first, open symbols to the second run of adsorption.

in comparison with Fig. 5a): this indicates that the interaction of NH_3 *via* a hydrogen bond with the SiOH groups is dominant. For instance, at an equilibrium pressure of 60 Torr the amounts adsorbed on Sil-A are twice as large as the amounts adsorbed on Sil-B (1.8 and 0.9 mmol g^{-1}, respectively). At the early stage of the adsorption process (P_{NH_3} = 1 Torr) the amount adsorbed on Sil-A is even larger (three times) with respect to Sil-B. The shape of the isotherms is similar in both cases and does not tend to saturation at the final equilibrium pressure reached ($P_{NH3} \approx 70$ Torr), even if the heats of adsorption, at least in the case of Sil-B, at this final equilibrium pressure are very low (*vide infra*).

In Fig. 7a the heats of adsorption (first and second runs) of NH_3 on Sil-A and Sil-B samples are reported as a function of the amounts adsorbed. In all cases the curves exhibit a shape typical of heterogeneous surfaces: in fact the heat of adsorption decreases continuously with increasing surface coverage from an initial high value (q_0, extrapolated at zero coverage) down to quite low values. The zero coverage values are ≈100 kJ mol^{-1} for Sil-A and only 80 kJ mol^{-1} for Sil-B. In both cases, the zero coverage value is consistent with the heat values reported for a crystalline, highly hydroxylated non-porous SiO_2 sample, whereas (for Sil-A) the heat values at high coverage are unusually high, if compared to the values previously measured for both crystalline non-porous silicas.[12] By increasing P_{NH_3} in the case of Sil-A, the curve decreases quite smoothly down to *ca.* 40 kJ mol^{-1}, whereas in the case of Sil-B, the curve decreases more abruptly down to very low values (*ca.* 20–25 kJ mol^{-1}: a figure very similar to the heat of condensation of NH_3). This implies that in the 0–0.65 mmol g^{-1} (0–35 Torr) interval NH_3 interacts with the hydroxyl groups of the nests of the Sil-B sample, while for $n_{ads} > 0.65$ mmol g^{-1} ($P_{NH3} > 35$ Torr) ammonia is physically adsorbed forming hydrogen-bonded NH_3 multilayers. As q_{ads} of NH_3 on Sil-A is always distinctly larger than the heat of condensation of NH_3, it is inferred that the hydroxyl groups are acting as adsorption centres in the whole $0 < n_{ads} < 2$ mmol g^{-1} ($0 < P_{NH_3} < 70$ Torr) interval and that they are not totally consumed even at $n_{ads} = 2$ mmol g^{-1} ($P_{NH_3} = 70$ Torr). This in turn implies that the silanol concentration, per unit mass of the sample, is at least three times larger than that on Sil-B. Note that this volumetric–calorimetric datum agrees well with the IR spectra reported in Fig. 4a (Sil-A), where a component, due to SiOH groups not interacting with ammonia, is still present even at the highest equilibrium pressures and with the same IR experiment performed on Sil-B (Fig. 5a) resulted in a complete perturbation of the ν(OH) of all SiOH groups by NH_3.

Notice also that in Sil-A the first and second run curves are virtually perfectly overlapped, whereas in the case of Sil-B, the first and second run curves are not perfectly overlapped, particularly at high coverage. Another peculiar feature of the heat curve of this latter sample is the apparent irregularity in the shape, indicating that the interaction of the probe molecule with the sites follows a non-simple mechanism. In fact, an evident discontinuity of q_{ads} *vs.* n_{ads} is observed around $n_{ads} \approx 0.6$ mmol g^{-1}, corresponding to $P_{NH_3} \approx 30$ Torr. The most striking results deriving from the comparison of the data in Fig. 7 is that the energy of interaction of NH_3 with the two silicalite samples is dramatically different over the whole coverage interval examined, as indicated by either the heat of adsorption *vs.* coverage (Fig. 7a), or equilibrium pressure (Fig. 7b) plots.

In Fig. 8 the integral heat evolved during the adsorption of increasing amounts of ammonia is reported. This plot indicates again that the evolution of heat upon increasing the amount of NH_3 adsorbed on the Sil-B sample becomes lower and lower with respect to that observed on Sil-A. In this latter case the coverage attained is much higher than in the former one (as already shown by the volumetric isotherms in Fig. 6, *vide supra*). This result cannot be explained only in terms of the higher concentration of hydroxyl groups present in Sil-A, because the number of sites is expected to influence mainly the amount of adsorbed NH_3 and not the differential heat of adsorption. We think that the explanation can be found when the organisation of silanols in the nests is considered. In Sil-A (characterised by a high concentration of hydroxyl groups) the silanols interact together *via* hydrogen bonds forming long linear chains or rings. On Sil-B the chains are shorter and the relative concentration of linear and cyclic chains must be different. The different situations can have a deep influence on the heat of adsorption. We shall return to this point in the next paragraph, where it will be shown that the heat of adsorption of NH_3 on terminal groups depends upon the length of the chain and is larger than the heat of adsorption on an isolated silanol. In this study the interaction of NH_3 (which can act as a H-bond donor and acceptor) with internal groups of the linear

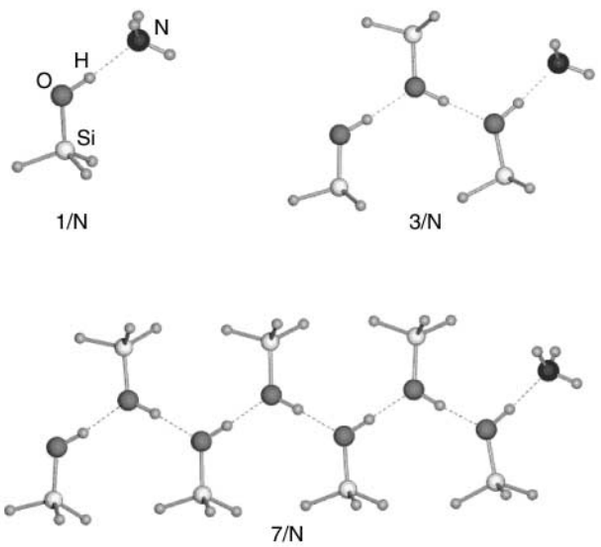

Fig. 9 Chains of interacting silanol molecules binding one NH_3 molecule at the terminal OH group. For the sake of brevity, beside isolated silanols, only chains with three and seven silanol molecules are shown. Geometries have been fully optimized at B3-LYP/6-31+G(d,p) within the C_s symmetry constraint.

chain is not considered in detail. However, we shall see in the next paragraph that the same process, involving small cyclic chains, can be accompanied by the release of high heat values, so partially justifying the remarkable high heats of desorption observed on Sil-A even at high NH_3 coverages.

Computational study of chains of interacting silanols

It has been shown that chains of interacting silanols can be used as a good model to explain both the IR spectroscopy[7] and the energetics[12] of the adsorption of ammonia on a fully hydoxylated silica surface. We will use the same model for describing "open" chains of silanols in the defective silicalite. By open we mean non-closed in a loop (*vide infra* next section).

The structural model adopted for the simulation of a fully hydroxylated silica surface consists of a chain of variable length made of isolated silanols (H_3SiOH) free to interact *via* H-bonding (see Fig. 9). The different number of silanols (from 1 to 7) mimics the different lengths of such chains on the real surface in which structural features dictate the extension of the chain itself. The growing number of silanol groups in a given chain modulates the increased ability of the terminal free hydroxyl group to be engaged in H-bonding interactions with NH_3. In that respect, we computed a binding energy of 35.5 kJ mol^{-1} for NH_3 interacting with a single silanol, which increases to 47.7 kJ mol^{-1} for the three membered chain and reaches an extrapolated value of 52.8 kJ mol^{-1} for a chain with an infinite number of silanol molecules.

As this data shows, the ability of the terminal OH group of the chain to form H-bonding interactions is enhanced by the cooperativity of the intra-chain H-bonds and can explain why, at low coverage, the heat of adsorption on Sil-A is distinctly higher than 35 kJ mol^{-1} so partially justifying the remarkably high heat of adsorption observed on Sil-A even at high NH_3 coverages. This effect is however already recovered by a simple three membered chain, because the resulting binding energy with respect to the adsorption of NH_3 is already 90% of the datum resulting from an infinite long chain in which co-operative effects are at their maximum. Considering that very long chains are improbable on a real surface, we can assume a three membered chain as a reasonable compromise to model a surface of interacting hydroxyls in defective silicalite.

Vibrational data enforce the proposed view. Indeed, the frequency red shift $\Delta\nu$(OH) suffered by the terminal OH bond

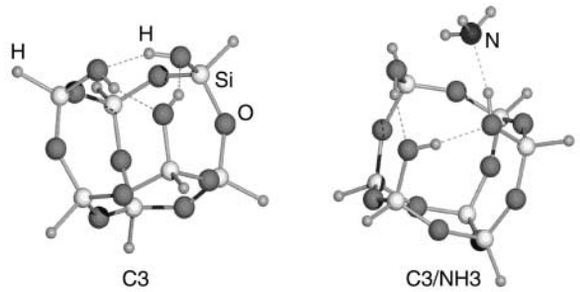

Fig. 10 Hydroxyls nest in a cluster model of a secondary building unit of silicalite either free (C3) and in interaction with the NH_3 molecule ($C3/NH_3$). Geometries have been fully optimised without constraints at the B3-LYP/6-31+G(d,p) level.

with respect to the value of the free silanol as due to the H-bond with the NH_3 molecule increases from almost -500 cm^{-1} for a single silanol/NH_3 case to -700 cm^{-1} for a chain of three silanols and reaches a value of -768 cm^{-1} as extrapolated datum for an infinitely long chain of silanol molecules. The $\Delta\nu$(OH) value of -700 cm^{-1} is already 93% of the maximum shift, in agreement with the behaviour showed by the energetic data. Both energetic and spectroscopic values are in fair agreement with the experimental results (*vide supra*).

Computational study of rings of interacting silanols

We have shown (*vide supra*) that, when the silicalite framework loses a Si atom from its structure, hydroxyl groups may act as repairing terminal groups, giving rise to a nest of hydroxyls in a mutual H-bonding interaction. On a microporous material such defects may also appear at the surface of the internal pores, giving rise to three interacting OH groups bound to Si atoms belonging to secondary building units of the silicalite framework. In Fig. 10 a cluster model is shown which has been adopted for such a secondary building unit in which a terminal SiOH group has been removed and a three membered hydroxyls nest is formed. Because of the defect's topology, the OH groups are buried within the ring of intra H-bonds so that no terminal OH groups are available for interaction with probe molecules. However, when the probe molecules can act as both an acceptor and donor of H-bonds as in the case of NH_3, the probe can enlarge the ring of interacting OH groups, acting as an extra moiety within the ring of H-bonded groups, as shown in Fig. 10. At variance with the case previously described for NH_3 interacting with a linear chain of interacting silanols, the process of insertion of NH_3 within the hydroxyls nest envisages an endothermic reaction, because of the breaking of the H-bonding nest. This energy cost is more than recovered by the energy gain resulting from the very strong cooperative effect within the $OH\cdots NH_3\cdots OH$ ring, resulting in a net binding energy of 57 kJ mol^{-1}. This datum is larger than the binding energy of NH_3 on an infinite chain of interacting silanols and shows, within the limits of the adopted clusters, that H-bonding cooperativity is greatly enhanced in a ring topology of only a few hydrogen bonds when compared to the corresponding linear chain of the same nuclearity. It is however of note that, the clusters used for modeling the internal OH ring (C3 and C3/NH3, see Fig. 10) are totally free to relax their geometry, in order to minimise the energy. The same will not occur for a hydroxyl nest inside the zeolite framework, because of the strain forces due to structural constraints. One should also note that the same constraints are less relevant for the linear chains, discussed in the previous paragraph, due to the higher flexibility of the framework at the surface. This fact can bias the energetics between linear and cyclic models interacting with ammonia so that more accurate calculations are needed to clarify this point.

The computed vibrational data show some interesting features which were absent for the case of NH_3 interacting with the linear chain of silanols. First of all, the $\Delta\nu$(OH) shift

suffered by the OH bond directly linked with the NH_3 molecule is -1038 cm^{-1}, a value which is remarkably larger than that computed for the terminal OH frequency of an infinite long chain. If we consider that on both Sil-A and Sil-B bands characterised by similar shifts have been observed, we conclude that in both samples closed rings of silanols are present, and that the relative concentration of rings is higher in Sil-B. Of course also in this case structural strain may play a role.

Conclusions

The synthesis method developed in EniChem laboratories[4] allows us to obtain a family of chemically very pure and structurally defective, silicalite samples. The internal defects in silicalite (generated by Si vacancies) are covered by hydroxyl groups (hydroxyl nests). These porous materials are characterised by defect concentrations (and hence hydroxyl nests) varying with continuity in a wide interval. In the present study we have focused our attention on two samples which are representative of two limiting situations in defect concentration.

On highly defective silicalites (Sil-A) the hydroxyl groups covering the walls of the nanovoids form linear and cyclic hydrogen-bonded chains, the linear chains being definitively more abundant. In low defective silicalites (Sil-B) the internal defects (diluted in the hydrophobic silicalite matrix) have smaller dimensions and the hydroxyl groups form preferentially ring chains of a small dimension.

Ammonia interacts preferentially with hydroxyl groups of the nests *via* hydrogen-bonds. The spectroscopic and energetic effects, either measured or calculated, are found to depend upon the hydroxyl group organisation in the nest. The spectroscopic effects associated with ammonia adsorption on the most defective samples are similar to those found on fully hydroxylated (non-porous) silica. The IR spectra of ammonia adsorbed on less defective silicalites can be interpreted and calculated on the basis of the interaction of NH_3 in the small rings of interacting hydroxyls covering the silica vacancies.

This combined neutron diffraction, spectroscopic (IR) and microcalorimetric study of adsorbed NH_3, supported by quantum chemical computation has elucidated the role of cooperative effects in hydrogen bonded chains and rings of silanols covering the internal defective nanocavities, explaining the remarkably higher adsorptive properties of this defective material with respect to perfect silicalite.[1] This study has provided an explanation for the reason why defective silicalites are hydrophilic materials (note that perfect silicalite is a hydrophobic and inert material). We can so explain the efficient and selective action of defective silicalites as a weakly acidic catalyst for the Beckman rearrangement reaction in terms of the presence of nests of cooperatively interacting silanols, hosted in the inert matrix of microporous silicalite.

Experimental

Neutron diffraction

Data were collected at the High Resolution Powder Diffraction instrument (HRPD: $\Delta d/d \approx 4$–5×10^{-4}) at ISIS (Didcot, UK) for 24 hours in order to obtain high-quality statistics. Approximately 3 cm^3 of defective silicalite (dehydrated form) were loaded in a sealed glass sample holder. Two ZnS scintillator banks at 168° and 90° with respect to the incident beam were used, giving rise to two independently measured powder patterns that have been simultaneously used in the structural Rietveld refinement. More details on both the experimental and the refinement strategies can be found in ref. 6.

IR

The IR spectra were obtained at room temperature on a Bruker IFS66 FTIR spectrometer equipped with a HgCdTe cryo-detector. Thin pellets of compressed powder were inserted in an all quartz IR cell permanently connected to a high vacuum manifold allowing *in situ* degassing procedures, gas dosages and measurements to be made.

Microcalorimetry

The heats of adsorption were measured at 303 K by means of a heat-flow microcalorimeter (Tian-Calvet type, Setaram-France) following a well-established stepwise procedure, previously described in ref. 13. The calorimeter was connected to a high vacuum gas-volumetric glass apparatus, that enabled the simultaneous determination of the amounts adsorbed and the heats evolved for small increments of the adsorptive. A first run of adsorption was performed on the samples previously outgassed at 673 K ($P \approx 10^{-4}$ Torr). A second run was performed after outgassing the sample overnight at the calorimeter temperature (303 K, $P \approx 10^{-5}$ Torr), in order to check the reversibility (under the adopted conditions) of the interaction. The pressure was monitored by means of a transducer gauge (Barocell 0–100 Torr, Edwards).

Computational methods

All calculations have been run at the *ab initio* level using the Gaussian-98 computer code[14] on model clusters apt to mimic surface silanols in different environments, either free or interacting with a single ammonia molecule. Geometries and vibrational frequencies in the harmonic approximation of the clusters both free and interacting with NH_3 have been computed at the B3-LYP/6-31+G(d,p) level, which has been shown to be a very good compromise between computational efficiency and chemical accuracy.[15] The unfilled valencies of the considered clusters are saturated by hydrogen atoms, following a standard recipe.[10] The interaction energies of NH_3 with different clusters have been computed in a supermolecular approach by considering, in all cases, the basis set superposition error.

Acknowledgements

The authors are grateful to L. Dalloro (EniChem, Istituto Guido Donegari in Novara, Italy) for fruitful discussion. IR and microcalorimetric measurements have been performed by C. Busco during her degree thesis in chemistry. The present work is part of a project coordinated by A. Zecchina and co-financed by Italian Murst (cofin 1998 area 03). The SERC is acknowledged for neutron beamtime at ISIS. The experiment (RB 8702) was partially supported by a grant under the CNR-SERC agreement. General financial support was provided by Italian CNR and MURST through research grants to G. A. R. Ibberson kindly helped with data collection.

References

1 (*a*) R. W. Grose and E. M. Flanigen, *US Pat.*, 4061724, 1977; (*b*) E. M. Flanigen, J. M. Bennett, R. W. Grose, J. P. Choen, R. L. Patton, R. M. Kirchner and J. V. Smith, *Nature*, 1978, **271**, 512.

2 ZSM-5 is a silicon-rich zeolite with an MFI structure (IUPAC nomenclature, see *e.g.* W. M. Meier, D. H. Olson and Ch. Baerlocher, *Atlas of Zeolite Structure Types*, Elsevier, London, 1996) showing a three-dimensional pore system consisting of two intersecting sets of tubular channels (*ca.* 5.5 Å in diameter) defined by 10-member rings of TO_4 tetrahedra.

3 (*a*) A. Zecchina, S. Bordiga, G. Spoto, L. Marchese, G. Petrini, G. Leofanti and M. Padovan, *J. Phys. Chem.*, 1992, **96**, 4987; (*b*) A. Zecchina, S. Bordiga, G. Spoto, L. Marchese, G. Petrini, G. Leofanti and M. Padovan, *J. Phys. Chem.*, 1992, **96**, 4991; (*c*) A. Zecchina, S. Bordiga, G. Spoto, L. Marchese, G. Petrini, G. Leofanti, M. Padovan and C. Otero Areàn, *J. Chem. Soc., Faraday Trans.*, 1992, **88**, 2959; (*d*) G. L. Marra, G. Tozzola, G. Leofanti, M. Padovan, G. Petrini, F. Genoni, B. Venturelli,

A. Zecchina, S. Bordiga and G. Richiardi, *Stud. Surf. Sci. Catal.*, 1994, **84**, 559.
4 M. Taramasso, G. Perego and B. Notari, *US Pat.*, 4410501, 1983.
5 (*a*) H. Sato, N. Ishii, K. Hirose and S. Kakamura, in 'New Developments in Zeolite Science and Technology', *Proceedings of the 7th International Zeolite Conference*, Tokyo, Japan, 1986, eds. Y. Murakami, A. Iijima and J. W. Ward, Elsevier, Amsterdam; *Stud. Surf. Sci. Catal.*, 1986, **28**, 755; (*b*) G. P. Heitmann, G. Dahlhoff and W. F. Hölderich, *J. Catal.*, 1999, **186**, 12; (*c*) M. Kitamura, H. Ichihashi and H. Tojima, *Eur. Pat.*, 494.535, 1991.
6 G. Artioli, C. Lamberti and G. L. Marra, *Acta Crystallogr.*, *Sect. B*, 2000, **57**, 2.
7 S. Bordiga, P. Ugliengo, A. Damin, C. Lamberti, G. Spoto, A. Zecchina, G. Spanò, R. Buzzoni, L. Dalloro and F. Rivetti, *Top. Catal.*, in press.
8 (*a*) B. A. Morrow and I. A. Cody, *J. Phys. Chem.*, 1973, **77**, 1465; (*b*) B. A. Morrow and I. A. Cody, *J. Phys. Chem.*, 1975, **79**, 761; (*c*) B. A. Morrow, *J. Phys. Chem.*, 1979, **81**, 2663; (*d*) P. Hoffmann and H. Knözinger, *Surf. Sci.*, 1987, **188**, 181; (*e*) V. Bolis, B. Fubini, L. Marchese, G. Martra and D. Costa, *J. Chem. Soc.*, *Faraday Trans.*, 1991, **87**, 497; (*f*) A. Zecchina, S. Bordiga, G. Spoto, D. Scarano, G. Spanò and F. Geobaldo, *J. Chem. Soc.*, *Faraday Trans.*, 1996, **92**, 4863; (*g*) C. Pazè, S. Bordiga, C. Lamberti, M. Salvalaggio, A. Zecchina and G. Bellussi, *J. Phys. Chem.*, 1997, **101**, 4741.
9 (*a*) G. C. Pimentel and A. McLellan, *The Hydrogen Bond*, ed. L. Pauling, W. H. Freeman, San Francisco, 1960; (*b*) H. Knözinger, in *The Hydrogen Bond*, eds. P. Schuster, G. Zundel and C. Sandorfy, North-Holland, Amsterdam, 1996, vol III, p. 1263; (*c*) H. Knözinger, in *Handbook of Heterogeneous Catalysis*, eds. G. Ertl, H. Knözinger and J. Weitkamp, Wiley-VCH, Weinheim, 1997, vol. 2, p. 707.
10 J. Sauer, P. Ugliengo, E. Garrone and V. R. Saunders, *Chem. Rev.*, 1994, **94**, 2095.
11 A. Zecchina, L. Marchese, S. Bordiga, C. Pazé and E. Gianotti, *J. Phys. Chem. B*, 1997, **101**, 10128.
12 (*a*) B. Fubini, V. Bolis, A. Cavenago and P. Ugliengo, *J. Chem. Soc.*, *Faraday Trans.*, 1992, **88**, 277; (*b*) B. Fubini, V. Bolis, A. Cavenago, E. Garrone and P. Ugliengo, *Langmuir*, 1993, **9**, 2712.
13 (*a*) V. Bolis, S. Bordiga, C. Lamberti, A. Zecchina, A. Carati, F. Rivetti, G. Spanò and G. Petrini, *Langmuir*, 1999, **15**, 5753; (*b*) V. Bolis, S. Bordiga, C. Lamberti, A. Zecchina, A. Carati, F. Rivetti, G. Spanò and G. Petrini, *Micropor. Mesopor. Mater.*, 1999, **30**, 67.
14 M. J. Frisch, G. W. Trucks, H. B. Schlegel, G. E. Scuseria, M. A. Robb, J. R. Cheeseman, V. G. Zakrzewski, J. A. Montgomery, Jr., R. E. Stratmann, J. C. Burant, S. Dapprich, J. M. Millam, A. D. Daniels, K. N. Kudin, M. C. Strain, O. Farkas, J. Tomasi, V. Barone, M. Cossi, R. Cammi, B. Mennucci, C. Pomelli, C. Adamo, S. Clifford, J. Ochterski, G. A. Petersson, P. Y. Ayala, Q. Cui, K. Morokuma, D. K. Malick, A. D. Rabuck, K. Raghavachari, J. B. Foresman, J. Cioslowski, J. V. Ortiz, A. G. Baboul, B. B. Stefanov, G. Liu, A. Liashenko, P. Piskorz, I. Komaromi, R. Gomperts, R. L. Martin, D. J. Fox, T. Keith, M. A. Al-Laham, C. Y. Peng, A. Nanayakkara, C. Gonzalez, M. Challacombe, P. M. W. Gill, B. Johnson, W. Chen, M. W. Wong, J. L. Andres, C. Gonzalez, M. Head-Gordon, E. S. Replogle and J. A. Pople, Gaussian 98, Revision A.7, Gaussian, Inc., Pittsburgh PA, 1998.
15 B. Civalleri, E. Garrone and P. Ugliengo, *J. Phys. Chem. B*, 1998, **102**, 2373.